Organic & Biomolecular Chemistry

www.rsc.org/obc

Volume 6 | Number 22 | 21 November 2008 | Pages 4069–4272

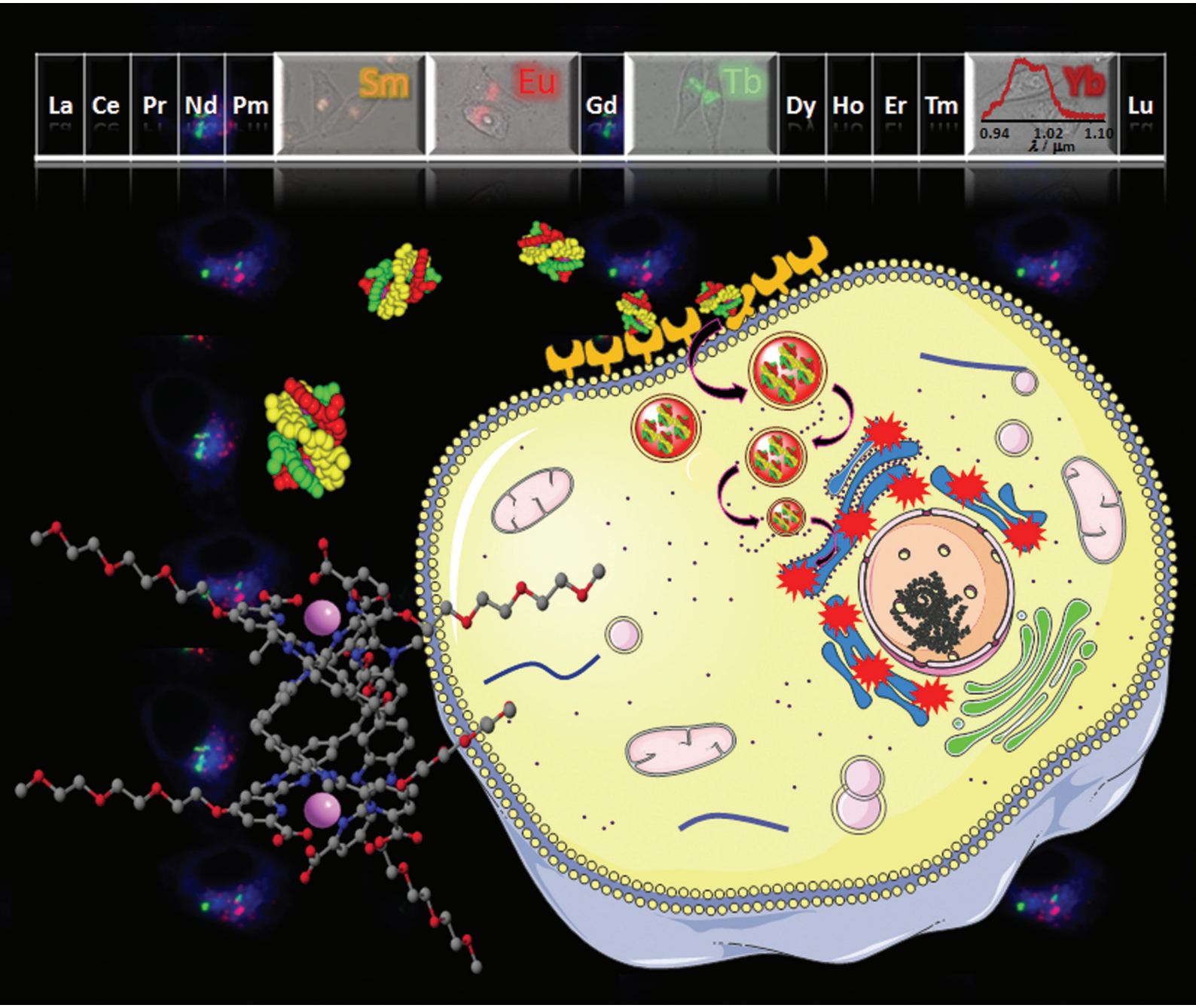

ISSN 1477-0520

RSC Publishing

FULL PAPER
Bo Song *et al.*
Time-resolved luminescence microscopy of bimetallic lanthanide helicates in living cells

EMERGING AREA
Katrina H. Jensen and Matthew S. Sigman
Mechanistic approaches to palladium-catalyzed alkene difunctionalization reactions

Time-resolved luminescence microscopy of bimetallic lanthanide helicates in living cells†

Bo Song, Caroline D. B. Vandevyver, Anne-Sophie Chauvin and Jean-Claude G. Bünzli*

Received 4th July 2008, Accepted 20th August 2008
First published as an Advance Article on the web 10th October 2008
DOI: 10.1039/b811427g

The cellular uptake mechanism and intracellular distribution of emissive lanthanide helicates have been elucidated by time-resolved luminescence microscopy (TRLM). The helicates are non-cytotoxic and taken up by normal (HaCat) and cancer (HeLa, MCF-7) cells by endocytosis and show a late endosomal–lysosomal cellular distribution. The lysosomes predominantly localize around the nucleus and co-localize with the endoplasmatic reticulum. The egress is slow and limited, around 30% after 24 h. The first bright luminescent images can be observed with an external concentration gradient of 5 μM of the Eu^{III} helicate [$Q = 0.21$, $\tau = 2.43$ ms], compared to >10 μM when using conventional luminescence microscopy. Furthermore, multiplex labeling could be achieved with the Tb^{III} [$Q = 0.11$, $\tau = 0.65$ ms], and Sm^{III} [$Q = 0.0038$, $\tau = 0.030$ ms] analogues.

Introduction

An important aspect of systems biology is the development of new, responsive, luminescent stains to probe the cellular environment.[1] Indeed, the development of new fluorescent dyes with improved photophysical properties, combined with the technical progress in optical devices for luminescence microscopy, open the way to superior fluorescence imaging technologies. As an alternative to classical organic fluorescent labels a new class of labeling agents, namely emissive lanthanide-complexes, emerged in the last decade.[2–4] The benefits of these are multiple as trivalent lanthanides (*e.g.*, Sm, Tb, Eu, Yb) show very interesting and specific luminescent properties: their luminescence is characterized by easily recognizable line-like emission spectra, long excited-state lifetimes (up to several milliseconds) allowing the use of time-resolved measurements,[5,6] and large Stokes shifts upon ligand excitation; this shift can be several hundred nanometres containing discrete gaps with zero absorption. In addition, lanthanide-containing stains display very small sensitivity to photobleaching in view of their ability to efficiently harvest energy from triplet states. Applications of lanthanide luminescence probes in time-resolved fluoro-immunoassays (TR-FIA) and DNA hybridization assays have been extensively investigated.[7–10] Recently, lanthanide complexes have been reported that are taken up by living cells and that can be visualized inside these cells by both gated and non-gated luminescence-based imaging techniques, such as classical confocal or epifluorescence microscopy,[11–20] time-resolved luminescence microscopy (TRLM),[21,22] or multiple-photon microscopy.[23–27] This led to the development of new responsive probes of the cellular environment[28,29] for parameters and analytes such as pH,[30,31] phospho-anions,[32] hydrogencarbonate,[33,34] singlet oxygen,[35] citrate,[29,36] and urate.[14,37]

During the past ten years, we have been tailoring homo-[38] and hetero-[39] bimetallic helicates with the overall composition $[Ln_2(L^{CX})_3]$ (see Scheme 1), with the final purpose of designing bi-functional lanthanide probes. More recently, we have demonstrated that upon adequate derivatization these bimetallic helicates are viable alternatives to the existing lanthanide chelates for live cell imaging.[17–19,40,41] In particular, $[Eu_2(L^{C2})_3]$ and $[Tb_2(L^{C2})_3]$ show large water solubility, high thermodynamic stability and kinetic inertness, sizeable luminescence quantum yields (21 and 11%), long lifetimes (2.43 and 0.65 ms), good cell permeability and non-cytotoxicity, which perfectly match the stringent requirements for a cell imaging probe.[40] Furthermore, these helicates provide a versatile platform for functionalization and targeting experiments, and although not yet taken advantage of, the intrinsic chirality of the helicates will be an asset in future developments of these probes. As we strive to develop luminescent lanthanide probes that can be targeted to certain compartments within the cell, we herein report the behavior of the $[Ln_2(L^{C2})_3]$ helicates as optical probes in TRLM of living cells, with emphasis on the elucidation of the process of cellular uptake and sub-cellular localization.

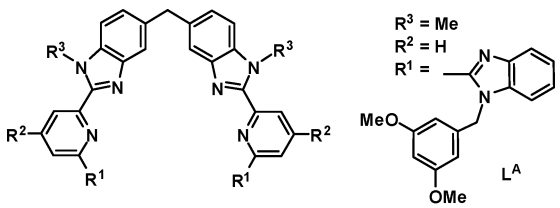

R^1	R^2	R^3	L
$CONEt_2$	H	Et	L^B
CO_2H	H	Et	H_2L^{C1}
CO_2H	$(OCH_2CH_2)_3OMe$	Me	H_2L^{C2}
CO_2H	H	$(CH_2CH_2O)_3Me$	H_2L^{C3}
$CONEt_2$	Cl	Et	L^E
$CONEt_2$	Br	Et	L^F
$CONEt_2$	NCS	Et	L^G

Scheme 1

Laboratory of Lanthanide Supramolecular Chemistry, École Polytechnique Fédérale de Lausanne, BCH 1404, 1015 Lausanne, Switzerland. E-mail: jean-claude.bunzli@epfl.ch

† Electronic supplementary information (ESI) available: Fig. S1. See DOI: 10.1039/b811427g

Methods

Cell lines and culture conditions

In this study the following cell lines were used: human cervical adenocarcinoma cell line HeLa (ATCC CCL-2), human breast adenocarcinoma cell line MCF-7 (ATCC HTB-22) and a non-malignant epithelial cell line HaCat (human keratinocytes). Cells were cultivated in 25 cm^2 culture flasks using RPMI 1640 (Sigma, R8758, UK) supplemented with 5% foetal calf serum (FCS), 2 mM L-glutamine, 1 mM sodium pyruvate, 1% non-essential amino-acids, 1% 4-(2-hydroxyethyl)piperazine-1-ethanesulfonic acid monosodium salt (HEPES) (all from Gibco® Cell Culture, Invitrogen, Basel, Switzerland). Cultures were maintained at 37 °C under 5% CO_2 and 95% air atmosphere. The growth medium was changed every other day until the time of use of the cells. Cell density and viability, defined as the ratio of the number of viable cells over the total number of cells, of the cultures were determined by trypan blue staining and a Neubauer improved hemacytometer (Blau Brand, Wertheim, Germany). Cell morphology was followed by means of a Zeiss luminescence microscope Axiovert 100 with contrast phase optics. For TRLM imaging experiments cells were seeded in glass bottom cell culture dishes obtained from MatTek Corporation (P35G-1.5–14-C, USA) or in plastic bottom µ-dishes Nr. 80136 from ibidi GmbH (Germany).

Preparation of lanthanide complexes

The luminescent lanthanide helicates, $[Eu_2(L^{C2})_3]$, $[Tb_2(L^{C2})_3]$ and $[Sm_2(L^{C2})_3]$, were synthesized and purified according to procedures described previously.[19]

Cell proliferation assay

Cell proliferation was measured with the WST-1 reagent (Cell Proliferation Reagent WST-1, Roche, Germany). HeLa cells were seeded in a 96-well tissue culture microplate at a concentration between 1–5 × 10^5 cells per well in 100 µL culture medium, and incubated overnight at 37 °C and 5% CO_2. Cells were treated with various concentrations of sodium iodoacetate (Acros, USA) in 100 µL per well culture medium at final concentration of 200, 100, 50, 25, 10, 0 µM for 2 h. 10 µL WST-1 reagent was added to each well and the plate was shaken for 1 min on a microtiter plate shaker (450 rpm). The plate was further incubated at 37 °C and 5% CO_2 for 2 h and the absorbance of the formazan product was measured at 450 nm with an ELISA reader (Spectra MAX 340, Molecular Devices, Sunnyvale, CA, USA). Cell viability was calculated from the absorbance values as follows:

$$\text{viability}_{\text{WST}}[\%] = \frac{\left(A_{450} - A_{650}\right)_{\text{exp}}}{\left(A_{450} - A_{650}\right)_{\text{medium}}} \times 100$$

with $A_{450} - A_{650}$ being the absorbance difference between 450 nm and 650 nm for the cells that were in contact with sodium iodoacetate ("exp") and the medium. Results are expressed as an averages over 3 nominally identical measurements.

Cell imaging

To detect the cellular uptake of the helicates, cells were seeded on a glass bottom cell culture dish (MatTek Corporation) or plastic bottom µ-dish (ibidi GmbH), loaded with the complex for a given time and then washed at least 5 times with phosphate buffered saline (PBS) 0.15 M, pH 7.4. Cells were examined with a Wallac Signifier TRLM from Perkin Elmer Analytical and Life Sciences consisting of a conventional luminescence microscope, Nikon Eclipse E600 coupled with a time-resolved work station.[42] The following measurement conditions were used; excitation: bandpass filter 340 (BP 70 nm); emission: longpass filter (LP) 420 nm; excitation pulse length: 10 µs; delay time: 100 µs (50 µs for Sm complexes); gate time: 600 µs; exposure time: 60 s. The Zeiss luminescence microscope Axiovert 100 was used with phase contrast optics for conventional luminescence imaging.

Co-localization experiments. (1) HeLa cells grown on a plastic bottom µ-dish were incubated with 100 µM $[Eu_2(L^{C2})_3]$ and 100 nM LysoTracker-blue DND-22 (Invitrogen™ Molecular Probes™, USA) at 37 °C and 5% CO_2 for 4 h. Luminescence of $[Eu_2(L^{C2})_3]$ within the cells was detected in TRLM mode and the fluorescence of the lysotracker dye was measured with conventional luminescence microscopy. (2) The cells grown on a plastic bottom µ-dish were incubated with 100 µM $[Eu_2(L^{C2})_3]$ at 37 °C and 5% CO_2 for 4 h. 1 µM ER-Tracker Blue-White DPX (Invitrogen™ Molecular Probes™, USA) was then added for an additional incubation of 30 min under the same conditions. Thereafter, 5 µM Golgi-Tracker, BODIPY® FL C_5-ceramide complexed to BSA (Invitrogen™ Molecular Probes™, USA) was added for 30 min at 4 °C. The luminescence of $[Eu_2(L^{C2})_3]$ within the cells was examined in TRLM mode and the fluorescence of the ER-Tracker Blue-White DPX and Golgi-Tracker dyes was collected with conventional luminescence microscopy.

Multiplex experiments. HeLa cells grown on a plastic bottom µ-dish were incubated with 100 µM $[Eu_2(L^{C2})_3]$ and 100 µM $[Tb_2(L^{C2})_3]$ at 37 °C and 5% CO_2 for 6 h. Luminescence of the lanthanide complexes within the cells was examined with TRLM using an appropriate emission filter, LP 585 nm for $[Eu_2(L^{C2})_3]$ and 545 nm (BP 35 nm) for $[Tb_2(L^{C2})_3]$.

Cell treatment protocols

Hypertonic sucrose treatment. HeLa cells were incubated at 37 °C and 5% CO_2 for 30 min with 0.45 M sucrose in the culture medium. After addition of 100 µM $[Eu_2(L^{C2})_3]$, cells were further incubated at 37 °C for 2 h before imaging.

Potassium depletion. HeLa cells were washed twice with the hypotonic medium (PBS–H_2O (1 : 3 v/v)) followed by a short 5 min incubation in the same medium. The cells were then washed 5 times in isotonic K^+-free Buffer A (100 mM NaCl and 50 mM HEPES at pH 7.4) followed by a 45 min incubation in the same medium. The latter was discarded and the cells were incubated with 100 µM $[Eu_2(L^{C2})_3]$ in Buffer B (100 mM NaCl, 50 mM HEPES, 1 mM $MgCl_2$, 1 mM $CaCl_2$ and 5% fetal calf serum at pH 7.4) for 2 h before imaging.

Metabolic inhibitors. HeLa cells were incubated at 37 °C and 5% CO_2 for 2 h in presence of sodium azide (0.1%) or sodium iodoacetate (IAA) at different concentrations in the culture medium; a concentration of 100 µM $[Eu_2(L^{C2})_3]$ was then added for an additional incubation of 4 h under the same conditions.

Time lapse experiments

HeLa cells grown on a plastic bottom μ-dish were incubated with 100 μM $[Eu_2(L^{C2})_3]$ at 37 °C and 5% CO_2 overnight. The medium was removed from the cell culture dish and the cells were washed 5 times with RPMI medium. The cells were placed at 37 °C and 5% CO_2 in a bulky volume of fresh RPMI medium and were used for TRLM at various time intervals.

Results

Cell morphology

HeLa cells grown in culture medium containing 100 μM $[Eu_2(L^{C2})_3]$ and examined in phase contrast mode by means of conventional luminescence microscope do not show any morphological difference with HeLa cells cultured in chelate-free medium (Fig. 1). After 7 h of incubation in the presence of the Eu bimetallic helicate, no swollen nuclei or visible granule were observed, although luminescence microscopy reveals that the cells contains a sizeable amount of $[Eu_2(L^{C2})_3]$ at this time and the viability of the cells was unchanged after 24 h. In contrast, when HeLa cells are incubated with acridine orange, a nucleic acid intercalating dye, swollen nuclei were visible in some cells after 7 h incubation and necrotic cells were clearly observed after 24 h incubation.[43] These results complement those obtained with the WST-1 assay[17] and indicate that the luminescent lanthanide helicates are non-cytotoxic and biocompatible for the sensing of targeted phenomena in living cells.

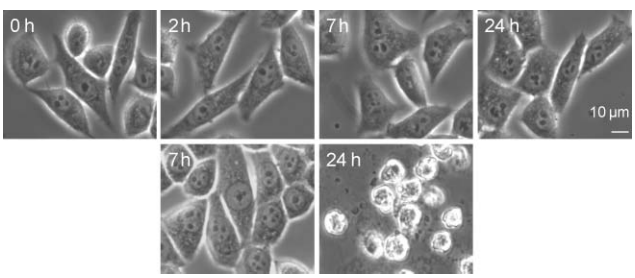

Fig. 1 Phase contrast photography of HeLa cells exposed to 100 μM $[Eu_2(L^{C2})_3]$ (top row) or 3.2 μM acridine orange (bottom row) at 37 °C and 5% CO_2 for the indicated time interval.

Distribution of $[Eu_2(L^{C2})_3]$ in living cells

We reported earlier that the bimetallic $[Eu_2(L^{C2})_3]$ helicate permeates into HeLa cells by endocytosis and stains their cytoplasm. Furthermore, the helicate remains undissociated in the cell as evidenced by *in cellulo* emission spectra and lifetime measurements.[40] Here, TRLM and a high amplifying objective lens (100×) were used to visualize the intracellular distribution of the $[Eu_2(L^{C2})_3]$ chelate. The luminescence lifetime of the $Eu(^5D_0)$ emitting level (2.43 ms) is considerably longer than the fluorescence lifetimes of organic compounds. Therefore, the use of TRLM enables the elimination of short-lived contributions from auto-fluorescence which results in an improved signal-to-noise ratio and increased sensitivity, compared to conventional luminescence microscopy (Fig. 2). HeLa cells grown on glass bottom cell culture dishes were incubated in cell culture medium with $[Eu_2(L^{C2})_3]$ at different

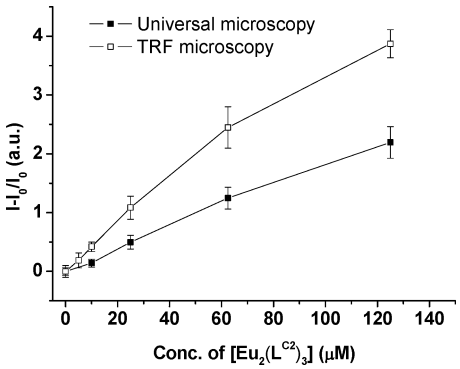

Fig. 2 Luminescence intensity of $[Eu_2(L^{C2})_3]$ in HeLa cells *versus* incubation concentration as measured by conventional luminescence microscopy (■, objective: Plan-Neofluar 40×, excitation filter = 330 nm (BP 80 nm), emission filter = LP 585 nm, exposure time 60 s) and time-resolved luminescence microscopy (□, objective: Plan-fluor 40×; excitation: 340 nm (BP 70 nm) filter; emission: 420 nm LP filter; excitation pulse length: 10 μs; delay time: 100 μs; gate time: 600 μs; exposure time: 60 s). I: luminescence intensity of cells loaded with $[Eu_2(L^{C2})_3]$; I_0: luminescence intensity of cell background.

concentrations for 6 h at 37 °C and 5% CO_2. Luminescence images of cells were taken using both non-gated and gated luminescence microscopy. The first bright luminescent images of cells were seen for complex loading concentrations >5 μM using TRLM compared to >10 μM for conventional luminescence microscopy.

The cellular uptake of the $[Eu_2(L^{C2})_3]$ helicates and their subsequent sub-cellular localization were further evaluated by TRLM at various incubation times after loading HeLa cells under cell culture condition at a chelate concentration of 100 μM (Fig. 3). It is clearly seen that after a short incubation time (15 min) the helicates are present in isolated vesicles which diffuse into the cytoplasm. After 1 h incubation, the majority of $[Eu_2(L^{C2})_3]$ complexes are located in a juxtanuclear area, in vesicles which cap the nucleus on one side of the cell. These vesicles show an almost continuous range in size from those that are barely visible to some as large as 2 μm but they are usually around 0.5–1.5 μm in diameter, and they commonly appear as flecks, spheres, or ellipsoids. It should be noted that even after 24 h incubation in the presence of the bimetallic complex, the helicates are still seen in the vesicles and do not diffuse into the cytoplasm or enter into the

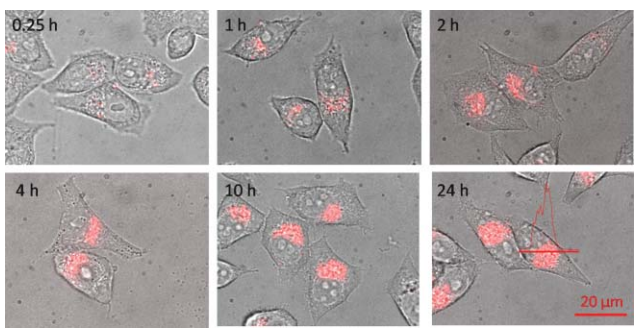

Fig. 3 HeLa cells were incubated in presence of 100 μM $[Eu_2(L^{C2})_3]$ in RPMI-1640 for 0–24 h at 37 °C. Then they were used for time-resolved luminescence imaging (objective: Plan-fluor 100×; excitation: 340 nm (BP 70 nm) filter; emission: 420 nm LP filter; excitation pulse length: 10 μs; delay time after excitation: 100 μs; gate time: 600 μs; exposure time: 30 s).

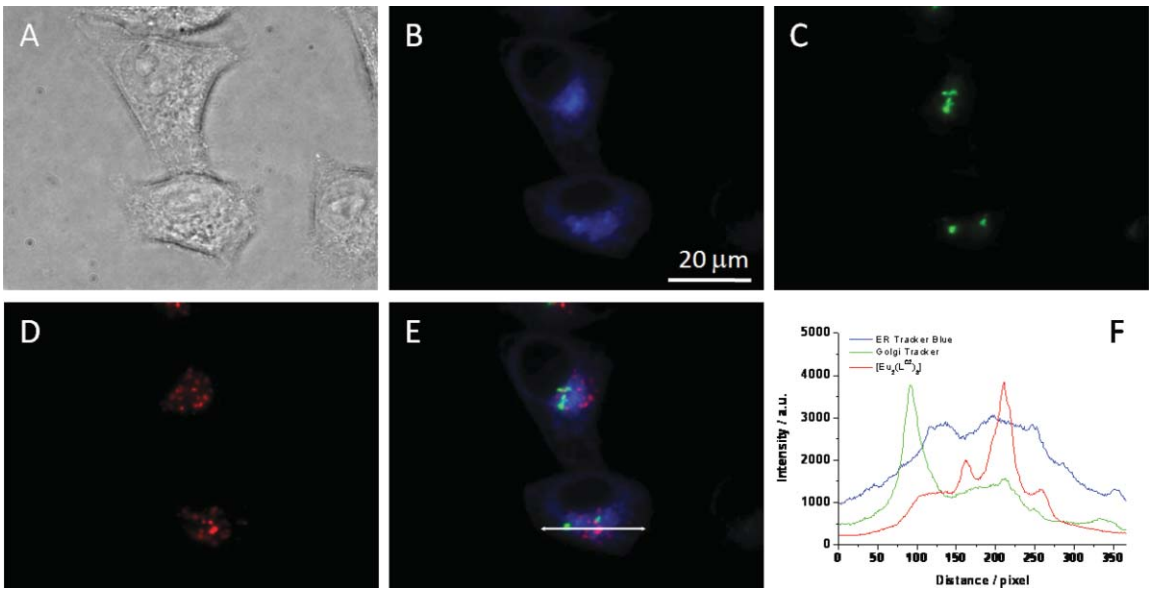

Fig. 4 Co-localization imaging of HeLa cells loaded with 100 µM $[Eu_2(L^{C2})_3]$ for 4 h and followed by a 30 min incubation with 1 µM ER-Tracker Blue-White DPX (at 37 °C) and a 30 min incubation with 5 µM Golgi-Tracker, BODIPY® FL C_5-ceramide complexed to BSA (at 4 °C). (A) Bright field; (B) fluorescence of ER-Tracker Blue-White DPX (objective: Plan-fluor 100×; excitation: 365 nm (BP 80 nm) filter, emission: 450 nm (BP 65 nm) filter, exposure time: 2 s); (C) fluorescence of Golgi-Tracker (objective: Plan-fluor 100×; excitation: 480 nm (BP 30 nm) filter, emission: 530 nm (BP 30 nm) filter, exposure time: 1.5 s); (D) Eu^{III} luminescence (excitation: 340 nm (BP 70 nm) filter; emission: 420 nm LP filter; excitation pulse length: 10 µs; delay time: 100 µs; gate time: 600 µs; exposure time: 30 s); (E) merged image. (F) Densitometric traces over the path shown in E.

nucleus. Co-localization experiments with the organic dyes ER-Tracker Blue-White DPX and Golgi-Tracker, BODIPY® FL C_5-ceramide, clearly showed that the majority of $[Eu_2(L^{C2})_3]$ stained vesicles localized within the endoplasmic reticulum, and not in the Golgi apparatus (Fig. 4).

Influence of endocytotic and metabolic inhibitors on cellular uptake

Observation of distinct vesicles in the cytoplasm of chelate-loaded cells points to an endocytotic process of cellular uptake of the bimetallic helicates. This was confirmed by the use of LysoTracker Blue dye, a fluorescent marker for secondary endosomes and lysosomes,[44] as well as endocytosis inhibitors.[45,46] In a first step, HeLa cells were simultaneously incubated with $[Eu_2(L^{C2})_3]$ and an organic marker before imaging by luminescence microscopy with appropriate filters and imaging mode (Fig. 5). The superimposed image 5D clearly shows the overlap of the red $[Eu_2(L^{C2})_3]$ luminescence with the blue fluorescence of the LysoTracker Blue dye, indicating the presence of the helicates into secondary endosomes and lysosomes. In a second series of experiments, the endocytotic uptake of the helicates by the cells was inhibited when the cells were exposed to a hypertonic medium (0.45 M sucrose): a 92% decrease in the uptake of the helicate by the cells was observed (Fig. 6).[45,46] The inhibiting effect of a hypertonic medium on receptor mediated endocytosis can be explained by (i) the fact that hypertonicity prevents the association between the receptor–ligand complex and the clathrin lattice to form a clathrin-coated pit, and (b) hypertonicity blocks receptor clustering which is necessary for the formation of the endosomes. It was also reported that receptor-mediated endocytosis in cultured fibroblasts can be subdued by depletion of intracellular K^+, which blocks the clathrin-coated pit formation.[47] After a hypotonic shock and K^+ depletion, the uptake of $[Eu_2(L^{C2})_3]$ into HeLa cells was severely inhibited, decreasing by 83% (Fig. 6). All these observations unambiguously prove that the helicates are internalized into the cells through a receptor-mediated endocytosis pathway.

The energy dependence of the helicate internalization process is also a good indication of its mechanism, so that the effects of metabolic inhibitors on the internalization of $[Eu_2(L^{C2})_3]$ were investigated. Sodium azide is widely used both *in vivo* and *in vitro* as an inhibitor of cellular respiration. It acts by blocking cytochrome C oxidase, the last enzyme in the mitochondrial electron transport chain, and thereby produces a drop in intracellular ATP concentration.[48] The uptake of the helicates into HeLa cells pretreated with sodium azide was significantly reduced to 65% of the control (Fig. 7).

Iodoacetic acid (IAA) is reported as a classical inhibitor of anaerobic glycolysis which is the main process involved in the production of ATP caused by hypoxia, acting primarily on the enzyme glyceraldehyde-3-phosphate dehydrogenase.[49] To investigate the relationship between the cell viability and the uptake of $[Eu_2(L^{C2})_3]$, HeLa cells were pretreated with sodium iodoacetate at different concentrations and cell proliferation was assessed by the WST-1 assay. The uptake of $[Eu_2(L^{C2})_3]$ by pretreated cells was estimated by TRLM. It was apparent that the internalization of $[Eu_2(L^{C2})_3]$ depends on the cell viability, the higher the cell proliferation, the more uptake of the helicate (Fig. 8). Altogether, these results suggest that the uptake of the Eu-helicate by living HeLa cells occurs through an energy-dependent and viability-dependent process and that the helicates are stored in the endosomes and lysosomes.

Fate of the luminescent stain after internalization

An important issue during the development of a cell-imaging probe is to determine the fate of the luminescence complex

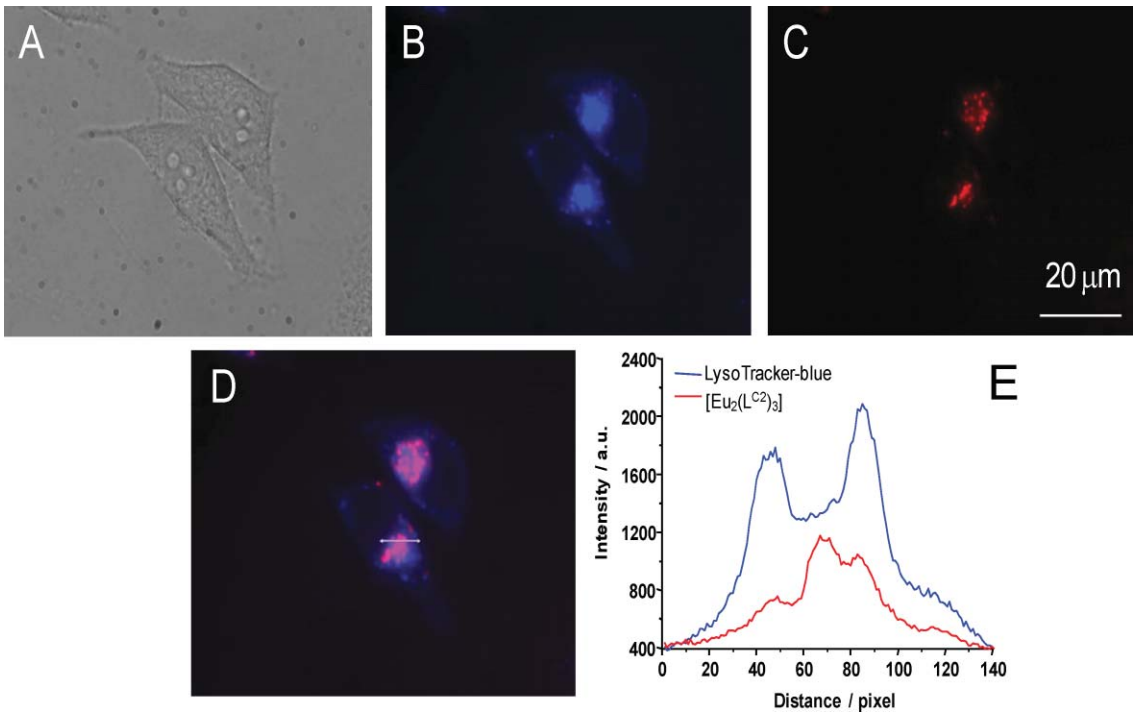

Fig. 5 Co-localization imaging of HeLa cells loaded with 100 μM $[Eu_2(L^{C2})_3]$ and 100 nM LysoTracker-blue DND-22 together for 4 h. (A) Bright field; (B) fluorescence of LysoTracker-blue DND-22 (objective: Plan-fluor 100×; excitation: 365 nm (BP 80 nm) filter, emission: 450 nm (BP 65 nm) filter, exposure time: 2 s); (C) Eu^{III} luminescence recorded in TRLM mode (objective: Plan-fluor 100×; excitation: 340 nm (BP 70 nm) filter; emission: 420 nm LP filter; excitation pulse length: 10 μs; delay time: 100 μs; gate time: 600 μs; exposure time: 60 s); (D) merged image. (E) Densitometric traces over the path shown in D.

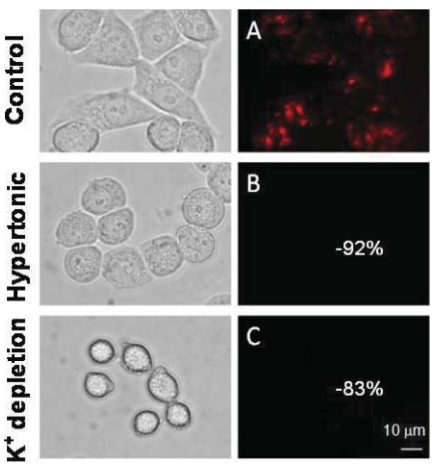

Fig. 6 Effects of endocytotic inhibitors on the internalization of $[Eu_2(L^{C2})_3]$ by HeLa cells. Left column: bright field; right column: luminescence images of cells incubated with the control medium (A), hypertonic sucrose medium (B) or potassium-depleted medium (C). Imaging conditions: objective: Plan-fluor 40×; excitation: 340 nm (BP 70 nm) filter; emission: 420 nm LP filter; excitation pulse length: 10 μs; delay time: 100 μs; gate time: 600 μs; exposure time: 60 s.

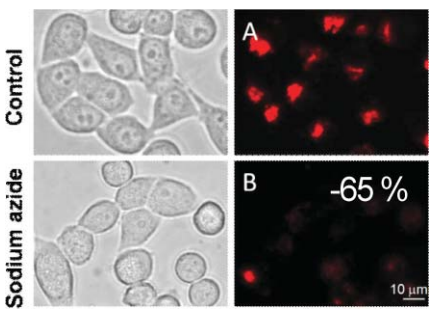

Fig. 7 Effect of sodium azide on the internalization of $[Eu_2(L^{C2})_3]$ by HeLa cells. Left column: bright field; right column: luminescence images of cells incubated with the control medium (A), 0.1% sodium azide medium (B). Imaging conditions: objective: Plan-fluor 40×; excitation: 340 nm (BP 70 nm) filter; emission: 420 nm LP filter; excitation pulse length: 10 μs; delay time: 100 μs; gate time: 600 μs; exposure time: 60 s.

after internalization by the cells. We previously showed that the $[Eu_2(L^{C2})_3]$ helicate survives un-dissociated in the cells, even at very low intracellular concentrations (7.9×10^{-16} mol of $[Eu_2(L^{C2})_3]$ per cell).[19] The leakage of the $[Eu_2(L^{C2})_3]$ helicate out of loaded cells has been assessed by a time-lapse experiment: HeLa cells were loaded with 100 μM of the $[Eu_2(L^{C2})_3]$ for 16 h and washed five times with the cell culture medium before being placed into a large volume of fresh helicate-free medium at 37 °C and 5% CO_2. TRLM images were recorded at various time intervals. As shown in Fig. 9, some $[Eu_2(L^{C2})_3]$ leaks out of the cells with increasing incubation time. However, the leakage of the helicates remains low and slow. When the total emitted intensity was monitored over one day, an intensity loss of less than 30% was recorded after 24 h. Furthermore, the helicates did not spread into the cytoplasm

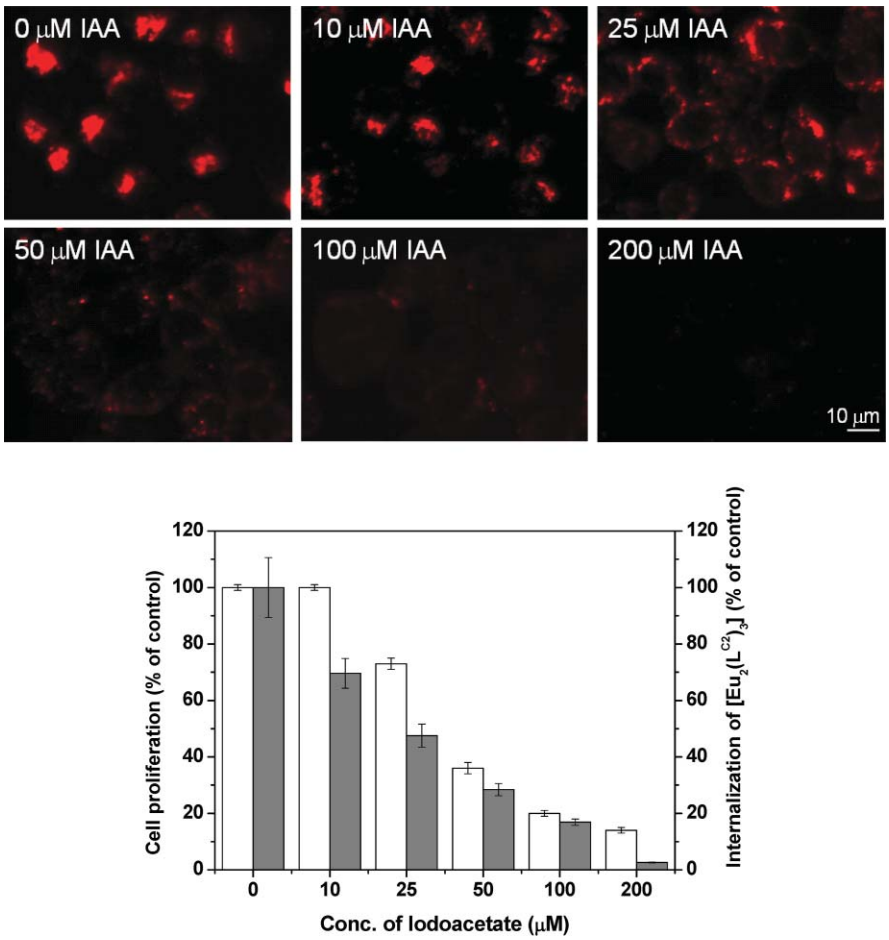

Fig. 8 Effect of iodoacetic acid on cellular uptake of $[Eu_2(L^{C2})_3]$ by HeLa cells. (Top) time-resolved luminescence images of HeLa cells pretreated with different concentrations of sodium iodoacetate and then loaded with 100 μM $[Eu_2(L^{C2})_3]$ for 4 h. (objective: Plan-fluor 40×; excitation: 340 nm (BP 70 nm) filter; emission: 420 nm LP filter; excitation pulse length: 10 μs; delay time: 100 μs; gate time: 600 μs; exposure time: 60 s). (Bottom) WST-1 assay of HeLa cells incubated with increasing concentrations of IAA (white column) and internalization of $[Eu_2(L^{C2})_3]$ by HeLa cells as assessed by TRLM (gray column).

of the cell but remained confined in lysosomes located near the nucleus.

Multiplex labeling

The ligand L^{C2} is a good sensitizer of the luminescence of several Ln^{III} ions, such as Eu^{III}, Tb^{III}, and, to a lesser extent Sm^{III} and Yb^{III}, leading to supramolecular edifices with overall quantum yields in water at pH 7.4 of 21, 11, 0.38, and 0.15% respectively.[19] To test the feasibility of multiplex experiments, HeLa cells were loaded simultaneously with $[Eu_2(L^{C2})_3]$ and $[Tb_2(L^{C2})_3]$. As can be seen from Fig. 10 (top), the $[Tb_2(L^{C2})_3]$ helicate has the same intracellular distribution as $[Eu_2(L^{C2})_3]$ in the co-loaded cells. This tends to indicate that the fate of the internalized Ln^{III} chelates is not influenced by the nature of the lanthanide ions and that the structure of the ligand plays a key role. Even the weakly emitting Sm^{III} complex with a quantum yield of less than 0.4% could be detected by TRLM (Fig. 10, bottom), which opens the way for using the helicates in multiplex targeting studies in living cells based on differential time-resolved measurements since the lifetimes of the excited states differ appreciably with values decreasing from 2.43 ms for Eu^{III}, to 0.65 ms for Tb^{III}, and 30.4 μs for Sm^{III}.

Staining other cell lines

The versatility of the helicates is further demonstrated by their ability to stain other cell lines such as the human breast adenocarcinoma cell line MCF-7 and the non-malignant epithelial cell line HaCat (human keratinocytes) (Fig. 11). Luminescence images of $[Eu_2(L^{C2})_3]$ and densitometry measurements across cells show that the helicate distribution in these cell lines is the same as for HeLa cells; the helicate shows again a predominantly lysosomal distribution near the cell nucleus. Co-localization experiments with the ER-Tracker Blue-White DPX dye demonstrates the presence of $[Eu_2(L^{C2})_3]$-containing lysosomes in the endoplasmatic reticulum (Fig. S1, ESI†).

Discussion

The cellular localization study demonstrates that the helicate $[Eu_2(L^{C2})_3]$ is taken up by living cells through an energy-dependent and viability-dependent endosomal–lysosomal mechanism. In the

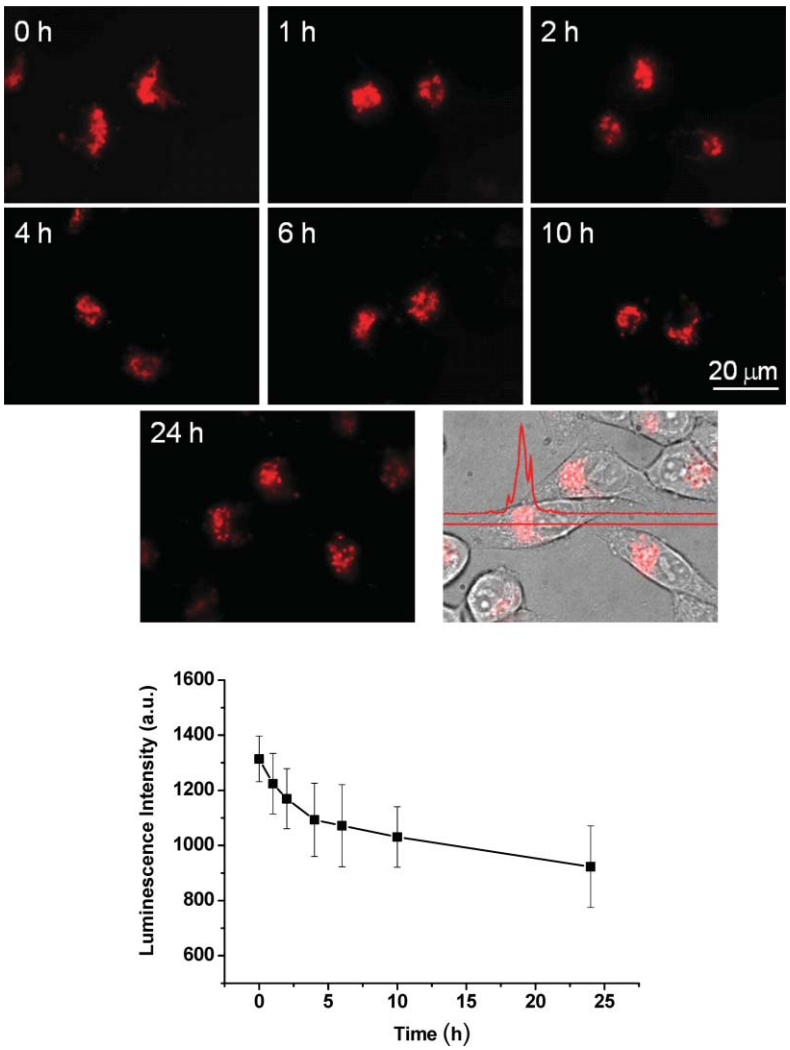

Fig. 9 Leakage of $[Eu_2(L^{C2})_3]$ from HeLa cells *versus* time. Cells were incubated 16 h at 37 °C with 100 μM $[Eu_2(L^{C2})_3]$, placed in a fresh Eu-free medium and maintained at 37 °C under 5% CO_2. (Top) TRLM images (objective: Plan-fluor 100×; excitation: 340 nm (BP 70 nm) filter; emission: 420 nm LP filter; excitation pulse length: 10 μs; delay time: 100 μs; gate time: 600 μs; exposure time: 30 s). (Bottom) leakage curves.

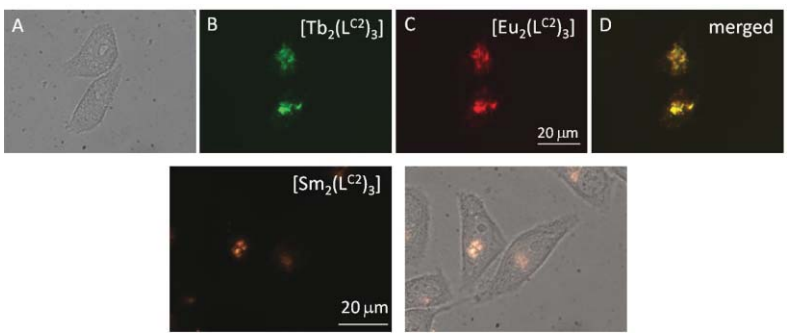

Fig. 10 Time-resolved luminescence images of living HeLa cells loaded with different Ln^{III} complexes. (Top) cells were incubated in presence of 100 μM $[Eu_2(L^{C2})_3]$ and $[Tb_2(L^{C2})_3]$ in RPMI-1640 for 6 h at 37 °C: (A) bright field; (B) Tb^{III} luminescence (excitation: 340 nm (BP 70 nm) filter; emission: 545 (BP 35 nm) filter; delay time: 100 μs; 60 s exposure time); (C) Eu^{III} luminescence (excitation: 340 nm (BP 70 nm) filter; emission: 585 nm LP filter; delay time: 100 μs; 60 s exposure time); (D) merged images. (Bottom) HeLa cells were incubated in presence of 500 μM $[Sm_2(L^{C2})_3]$ in RPMI-1640 for 24 h at 37 °C; left: Sm^{III} luminescence (excitation: 340 nm (BP 70 nm) filter; emission: 420 nm LP filter, delay time: 50 μs; 60 s exposure time); right: merged bright field/luminescence image.

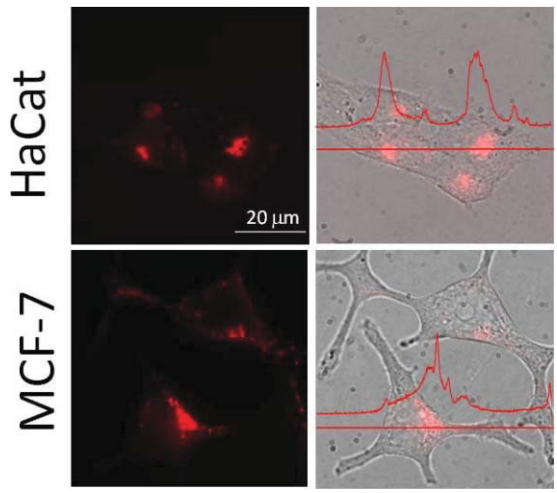

Fig. 11 Time-resolved luminescence images of HaCat (top row) and MCF-7 (bottom row) cells loaded with 100 µM $[Eu_2(L^{C2})_3]$ for 6 h at 37 °C. Left column: time-resolved luminescence images (objective: Plan-fluor 100×; excitation: 340 nm (BP 70 nm) filter; emission: 420 nm LP filter; excitation pulse length: 10 µs; delay time: 100 µs; gate time: 600 µs; exposure time: 30 s); right column: merged bright field and luminescence images.

presence of a sufficiently high external concentration gradient and especially at longer time intervals, the Eu^{III} bimetallic helicate is seen in late endosomes and lysosomes. The latter are predominantly distributed around the nucleus, co-localize with the endoplasmatic reticulum, and do not diffuse into the whole cells. The leakage of the helicate out of the cells is very slow and limited (30% after 24 h). This endosomal uptake mechanism of the helicate can be related to its relative high molecular weight ($[Eu_2(L^{C2})_3]$ ≈2827 Da) and electric neutrality. The macrocyclic cyclen-based lanthanide chelates, bearing azaxanthone, azathiaxanthone or tetrazatriphenylene chromophores, described by the group of David Parker, show different uptake and cellular localization profiles. These small, cationic complexes (MW ≈1000 Da) are entering living cells more rapidly (5–30 min), and most of them show a rapid egress; as these observations persist at 4 °C, an uptake mechanism involving a channel or pore in the cell membrane is proposed. Depending on the sensitizing chromophore, the macrocyclic complexes localize in different intracellular compartments. For instance, cationic or neutral Eu(III) complexes incorporating a coordinated azathioxanthone sensitizer, show a relatively slow uptake (>30 min) and leakage, and localize in the protein-rich regions of the nucleolus and ribosomes[15,30] or in the mitochondria;[16] complexes bearing a sensitizing azaxanthone group show a late endosomal–lysosomal distribution around the nucleus,[27] while cationic complexes which incorporate a tetraazatriphenylene moiety tend to penetrate (<15 min) and egress cells rapidly and localize inside the cell nucleus.[13] These results show that small changes in the sensitizing chromophore can alter the cellular uptake and localization of cyclen based Ln^{III} complexes, which makes the prediction of cellular uptake characteristics difficult for the time being in view of the limited set of data available.

We have previously evaluated the influence of the position and length of the polyoxyethylene substituents on the performance of the Eu helicates as imaging probes. The cellular endocytotic uptake mechanism and the localization were not altered by grafting the short polyoxyethylene chains on the benzimidazole cores of L^C,[18] or by doubling their length.[41] Other modifications of the core of the ditopic hexadentate ligand H_2L^{C2} are under way in our laboratories to further test a potential influence of the ligand structure on the uptake mechanism as well as for attempting to shift the excitation wavelength more towards the visible range.[50]

Conclusion

The experiments described in this work confirm that TRLM of living cells is instrumental in clearly separating the long-lived luminescence of lanthanide chelates from the short-lived autofluorescence present in most biological systems, the scattered excitation light, and even the fluorescence of organic dyes in co-localization experiments.

Another useful fact is that the bimetallic helicates $[Ln_2(L^{C2})_3]$ used in this study incorporate several requirements for live-cell imaging probes. In particular, an absence of cytotoxicity up to an external concentration gradient of 500 µM (that is, IC_{50} is >500 µM); in comparison, cyclen-based optical probes tend to be more cytotoxic, most of them having IC_{50} values for NIH-3T3 cells around 200 µM, but in some isolated cases IC_{50} is even smaller than 10 µM.[16,27] Furthermore, the helicates possess good cell permeability with slow egress. Finally, the sizeable luminescence sensitization reached for several Ln^{III} ions (Ln = Eu, Tb, Sm, and Yb) coupled with the derivatization potential of the polyoxyethylene pendant arms are promising for the development of time-resolved multiple targeting experiments both in the visible and near-infrared ranges. The robustness of the helicates makes them ideal probes for functionalization. For instance, coupling of the helicates *via* activated polyoxyethylene arms to specific biological molecules, such as peptides which permit endosomal escape (*e.g.* TAT peptide[48]), and antibodies, will allow the development of new molecular tracking and imaging agents. Their high specificity and attractive spectroscopic properties are hoped to bring to reality the following of discrete intracellular molecular events in real time.

Acknowledgements

This work is supported by grants from the Swiss National Science Foundation (200020_119866/1) and the Swiss Office for Science and Education (contract # SER C07.0116, under the frame of the ESF COST D38 Action). We thank Frédéric Gumy for his help with photophysical measurements.

References

1 N. Johnsson and K. Johnsson, *Chem. Biol.*, 2007, **2**, 31.
2 K. J. Franz, M. Nitz and B. Imperiali, *ChemBioChem*, 2003, **4**, 265.
3 B. R. Sculimbrene and B. Imperiali, *J. Am. Chem. Soc.*, 2006, **128**, 7346.
4 A. M. Reynolds, B. R. Sculimbrene and B. Imperiali, *Bioconjugate Chem.*, 2008, **19**, 588.
5 G. Vereb, E. Jares-Erijman, P. R. Selvin and T. M. Jovin, *Biophys. J.*, 1998, **74**, 2210.
6 A. Beeby, S. W. Botchway, I. M. Clarkson, S. Faulkner, A. W. Parker, D. Parker and J. A. G. Williams, *J. Photochem. Photobiol., B*, 2000, **57**, 83.
7 I. Hemmilä and V. M. Mukkala, *Crit. Rev. Clin. Lab. Sci.*, 2001, **38**, 441.
8 J. L. Yuan, G. L. Wang, K. Majima and K. Matsumoto, *Anal. Chem.*, 2001, **73**, 1869.

9 E. P. Diamandis and T. K. Christopoulos, *Anal. Chem.*, 1990, **62**, 1149.
10 E. Soini and T. Lövgren, *Crit. Rev. Anal. Chem.*, 1987, **18**, 105.
11 G. Bobba, J. C. Frias and D. Parker, *Chem. Commun.*, 2002, 890.
12 J. C. Frias, G. Bobba, M. J. Cann, C. J. Hutchison and D. Parker, *Org. Biomol. Chem.*, 2003, **1**, 905.
13 R. A. Poole, G. Bobba, M. J. Cann, J. C. Frias, D. Parker and R. D. Peacock, *Org. Biomol. Chem.*, 2005, **3**, 1013.
14 R. A. Poole, C. P. Montgomery, E. J. New, A. Congreve, D. Parker and M. Botta, *Org. Biomol. Chem.*, 2007, **5**, 2055.
15 J. H. Yu, D. Parker, R. Pal, R. A. Poole and M. J. Cann, *J. Am. Chem. Soc.*, 2006, **128**, 2294.
16 B. S. Murray, E. J. New, R. Pal and D. Parker, *Org. Biomol. Chem.*, 2008, **6**, 2085.
17 C. D. B. Vandevyver, A.-S. Chauvin, S. Comby and J.-C. G. Bünzli, *Chem. Commun.*, 2007, 1716.
18 A.-S. Chauvin, S. Comby, B. Song, C. D. B. Vandevyver and J.-C. G. Bünzli, *Chem.–Eur. J.*, 2007, **13**, 9515.
19 A.-S. Chauvin, S. Comby, B. Song, C. D. B. Vandevyver and J.-C. G. Bünzli, *Chem.–Eur. J.*, 2008, **14**, 1726.
20 F. L. Jiang, C. T. Poon, W. K. Wong, H. K. Koon, N. K. Mak, C. Y. Choi, D. W. J. Kwong and Y. Liu, *ChemBioChem*, 2008, **9**, 1034.
21 N. Weibel, L. J. Charbonnière, M. Guardigli, A. Roda and R. F. Ziessel, *J. Am. Chem. Soc.*, 2004, **26**, 4888.
22 L. J. Charbonniere, N. Hildebrandt, R. F. Ziessel and H. G. Loehmannsroeben, *J. Am. Chem. Soc.*, 2006, **128**, 12800.
23 G. L. Law, K. L. Wong, C. W. Y. Man, W. T. Wong, S. W. Tsao, M. H. W. Lam and P. K. S. Lam, *J. Am. Chem. Soc.*, 2008, **130**, 3714.
24 A. Picot, A. D'Aleo, P. L. Baldeck, A. Grichine, A. Duperray, C. Andraud and O. Maury, *J. Am. Chem. Soc.*, 2008, **130**, 1532.
25 A. D'Aléo, G. Pompidor, B. Elena, J. Vicat, P. L. Baldeck, L. Toupet, R. Kahn, C. Andraud and O. Maury, *ChemPhysChem*, 2007, **8**, 2125.
26 L. O. Palsson, R. Pal, B. S. Murray, D. Parker and A. Beeby, *Dalton Trans.*, 2007, 5726.
27 F. Kielar, G. L. Law, E. J. New and D. Parker, *Org. Biomol. Chem.*, 2008, **6**, 2256.
28 J.-C. G. Bünzli and C. Piguet, *Chem. Soc. Rev.*, 2005, **34**, 1048.
29 S. Pandya, J. H. Yu and D. Parker, *Dalton Trans.*, 2006, 2757.
30 R. Pal and D. Parker, *Org. Biomol. Chem.*, 2008, **6**, 1020.
31 R. Pal and D. Parker, *Chem. Commun.*, 2007, 474.
32 P. Atkinson, Y. Bretonniere and D. Parker, *Chem. Commun.*, 2004, 438.
33 Y. Bretonniere, M. J. Cann, D. Parker and R. Slater, *Chem. Commun.*, 2002, 1930.
34 Y. Bretonniere, M. J. Cann, D. Parker and R. Slater, *Org. Biomol. Chem.*, 2004, **2**, 1624.
35 B. Song, G. Wang, M. Tan and J. Yuan, *J. Am. Chem. Soc.*, 2006, **128**, 13442.
36 D. Parker and J. H. Yu, *Chem. Commun.*, 2005, 3141.
37 R. A. Poole, F. Kielar, S. L. Richardson, P. A. Stenson and D. Parker, *Chem. Commun.*, 2006, 4084.
38 M. Elhabiri, R. Scopelliti, J.-C. G. Bünzli and C. Piguet, *J. Am. Chem. Soc.*, 1999, **121**, 10747.
39 N. André, T. B. Jensen, R. Scopelliti, D. Imbert, M. Elhabiri, G. Hopfgartner, C. Piguet and J.-C. G. Bünzli, *Inorg. Chem.*, 2004, **43**, 515.
40 J.-C. G. Bünzli, A.-S. Chauvin, C. D. B. Vandevyver, B. Song and S. Comby, *Ann. N. Y. Acad. Sci.*, 2008, **1130**, 97.
41 E. Deiters, B. Song, A.-S. Chauvin, C. D. B. Vandevyver and J.-C. G. Bünzli, *New J. Chem.*, 2008, **32**, 1140.
42 L. Seveus, M. Vaisala, S. Syrjanen, M. Sandberg, A. Kuusisto, R. Harju, J. Salo, I. Hemmila, H. Kojola and E. Soini, *Cytometry*, 1992, **13**, 329.
43 E. Robbins, N. K. Gonatas and P. I. Marcus, *J. Cell Biol.*, 1964, **21**, 49.
44 W. Lu, Q. Sun, J. Wan, Z. J. She and X. G. Jiang, *Cancer Res.*, 2006, **66**, 11878.
45 G. Daukas and S. H. Zigmond, *J. Cell Biol.*, 1985, **101**, 1673.
46 J. E. Heuser and R. G. W. Anderson, *J. Cell Biol.*, 1989, **108**, 389.
47 J. M. Larkin, M. S. Brown, J. L. Goldstein and R. G. W. Anderson, *Cell*, 1983, **33**, 273.
48 V. P. Torchilin, R. Rammohan, V. Weissig and T. S. Levchenko, *Proc. Natl. Acad. Sci. U. S. A.*, 2001, **98**, 8786.
49 D. L. Foxall, K. M. Brindle, I. D. Campbell and R. J. Simpson, *Biochim. Biophys. Acta*, 1984, **804**, 209.
50 E. Deiters, B. Song, A.-S. Chauvin, C. D. B. Vandevyver, F. Gumy and J.-C. G. Bünzli, *Chem.–Eur. J.*, accepted for publication.